ISSN 1068-3739, Russian Meteorology and Hydrology, 2018, Vol. 43, No. 9, pp. 613–624. Allerton Press, Inc., 2018.
Original Russian Text S. Farhadipour, M. Azadi, A.A. Bidokhti, H. Sayyari, O. Alizadeh Choobari, 2018, published in Meteorologiya i Gidrologiya, 2018, No. 9, pp. 81–96.

Study and Simulation of Severe Dust Storms in the West and Southwest of Iran

S. Farhadipour[a]*, M. Azadi[b], A. A. Bidokhti[b], H. Sayyari[c], and O. Alizadeh Choobari[b]

[a]*Atmospheric Science & Meteorological Research Centre (ASMERC), Tehran, Iran*
[b]*Institute of Geophysics, University of Tehran, Tehran, Iran*
[c]*Supreme National Defense University, Tehran, Tehran, Iran*
**e-mail: saeed.farhadypoor@gmail.com*

Received August 3, 2016; in final form, March 19, 2017

Abstract—In recent decades, the number of dust events has increased significantly in the west and southwest of Iran. In this research, a survey on the dust events during the period 1990–2013 is carried out using historical dust data collected from seven synoptic stations scattered across the west and southwest of Iran. Using statistical analysis of the observational data, two of the most severe dust storm events that occurred in the region on July 4–7, 2009 and June 17–20, 2012 were selected and analyzed synoptically. NCEP/NCAR reanalysis dataset was used to obtain the required fields including sea level pressure, surface wind field, geopotential height at 500 hPa, and wind and vertical motion at the 850 hPa level. Moreover, weather research and forecasting model coupled with chemistry (WRF-Chem) with two aerosol schemes, GOCART and MADE/SORGAM, were used to simulate the amount of particulate matter (PM_{10}) and its transportation over the studied region. The initial and lateral boundary conditions of the model simulations are provided by Global Forecast System (GFS) data with the horizontal resolution of 0.5 . The calculations demonstrated that the MADE/SORGAM scheme predicted the values and trends of PM_{10} better than GOCART. Dust plums are formed over Iraq and Syria and then transported to the west and southwest of Iran. Comparing the MODIS satellite images for July 4, 2009 and June 18, 2012 with the corresponding model output showed the good performance of WRF-Chem in simulating the spatial distribution of dust.

DOI: 10.3103/S106837391809008X

Keywords: Dust storm, WRF-Chem model, MADE/SORGAM, GOCART, PM_{10}

1. INTRODUCTION

Dust events frequently occur in arid and semi-arid areas of the world. Northern Hemisphere generates around 90% of global airborne mineral dust, and there this dust is also deposited [2]. In Asia, a dust belt stretches from the Middle East (Jordan, Syria, Saudi Arabia, Iraq, Iran, Afghanistan, and Pakistan) through Central Asia (Turkmenistan and northern India) to the Tarim basin in China [10, 15, 25] and the Gobi Desert in Mongolia.

In recent years, dust events in the Middle East have attracted the attention of many scientists. Former studies about this region classified the regions in the Middle East according to the season of the greatest dust-raising activity [16]. Paper [16] showed that in the Lower Mesopotamian Plains the main seasons of dust storms were spring and summer. Paper [17] demonstrated that the highest frequencies occur at the convergence of borders between Iran, Pakistan, and Afghanistan. Paper [7] analyzed visibility reduction using eight "three-hour" mean values for each month for a 21-year period (1973–1993) and concluded that Iraq, Saudi Arabia, and the Persian Gulf were the regions reporting the highest occurrences of dust storms. Dust storms in Iran, northeastern Iraq, Syria, the Persian Gulf countries and the southern Arabian Peninsula were more frequent in summer, while they occurred mainly in spring in western Iraq, Syria, Jordan, Lebanon, the northern Arabian Peninsula, and southern Egypt [7].

Modeling heavy dust events to reach the accurate and timely prediction of this phenomenon can help not only to investigate the types of dust storms but also to produce their forecast and warnings. Numerical sim-

ulation of dispersion and transition of particulate matters is important to investigate dust raise from the surface and its motion in the atmosphere [19].

Various numerical schemes are accessible to simulate weather and atmospheric chemistry. These methods are used in the simulations of such processes as diffusion and ground deposition [29]. So, the coupling of meteorology and chemistry models provides more consistency between meteorological and chemical processes; it also allows considering the influence of the feedback effects mainly related to aerosol load [3, 11, 32].

The main advantage of online coupled meteorology and chemistry simulations is the account of aerosol concentration effects on meteorology [3]. In the Air Quality Models (AQMs) meteorology simulation outputs are used as the input of the model of the particulate matter in the atmosphere [3].

Observations show increase in dust events occurrence over the west and southwest of Iran during the past decade. As the most part of the surface in the Middle East is covered dominantly with alluvial plains and dry deserts with vast areas of unconsolidated sediments, aeolian processes are very important. In the west of Iran, there are Iran Highland and Zagros Mountains. The data on soil erosion in the southwestern part of Iran and satellite images indicate that the main sources of dust lie off the country borders, in Iraque, Syria, and the north of the Arabian Peninsula [34]. There are important and densely populated provinces in the west and southwest of Iran such as Khuzestan, Kermanshah, Ilam, Bushehr, and Kurdistan. There live about 17% of the Iran population, Sometimes the severity of dust events in this region is more than 10000 g/m^3 and is not recordable by conventional measurement instruments. During every heavy dust storm, hundreds of people rush to hospital for respiratory distress, airlines are forced to cancel their domestic flights, and social unrest and violence is spread in the region. Dust aerosols perturb the atmospheric radiation balance directly and indirectly; directly through scattering and absorbing by interacting both with short- and long-wave radiation [8, 23, 33] and indirectly by modifying cloud microphysics and cloud optical properties [14, 21].

The simulation and prediction of air quality is a complicated problem. Its solution involves both meteorological factors (e.g., wind speed and direction, turbulence, radiation, clouds, and precipitation) and chemical processes (e.g., deposition and transformations). Chemical and physical processes are coupled in the real atmosphere and are also connected to various meteorological processes such as radiation budget variations and the interaction of aerosols with cloud condensation nuclei (CCN) [12].

One of the difficulties in evaluating dust events is the lack of observational data with appropriate spatial and temporal resolution. The World Meteorological Organization (WMO) has a developed Aerosol Robotic Network (AERONET). Only one AERONET station is located in Iran. So, due to the extent of the dust phenomenon especially in western Iran, the expansion of this network may not be sufficient over the west of Iran.

The main objective of this study is to reveal the regional distribution of dust events in the west and southwest of Iran and analyze the capability of Weather Research and Forecasting model coupled with Chemistry (known as WRF-Chem) to predict the dust storm events that occurred in the west and southwest of Iran during July 4–7, 2009 and June 17–20, 2012.

2. THE SPATIAL AND TEMPORAL CHARACTERISTICS OF DUST STORMS IN THE WEST AND SOUTHWEST OF IRAN

In the present study, we use three-hourly surface meteorological reports from seven weather stations for a period of 24 years (1990–2013) (Fig. 1) to analyze the synoptic features of the dust events that occurred in the west and southwest of Iran. The stations are located at the entrance gate of dust events from Iraq, Syria, and the north of Arabian Peninsula

Based on the WMO protocol, dust events are classified into the following categories:

—dust-in-suspension, DIS: widespread dust is in suspension but is not raised at the station or near it at the time of observation; visibility is usually not greater than 10 km;

—blowing dust, BD: raised dust or sand at the time of observation that reduces visibility (it is from 1 to 10 km);

—dust storm (DS): strong wind lifting great quantities of dust particles and reducing visibility between 200 and 1000 m;

—severe dust storm (SDS): very strong wind lifting large quantities of dust particles and reducing visibility to less than 200 m.

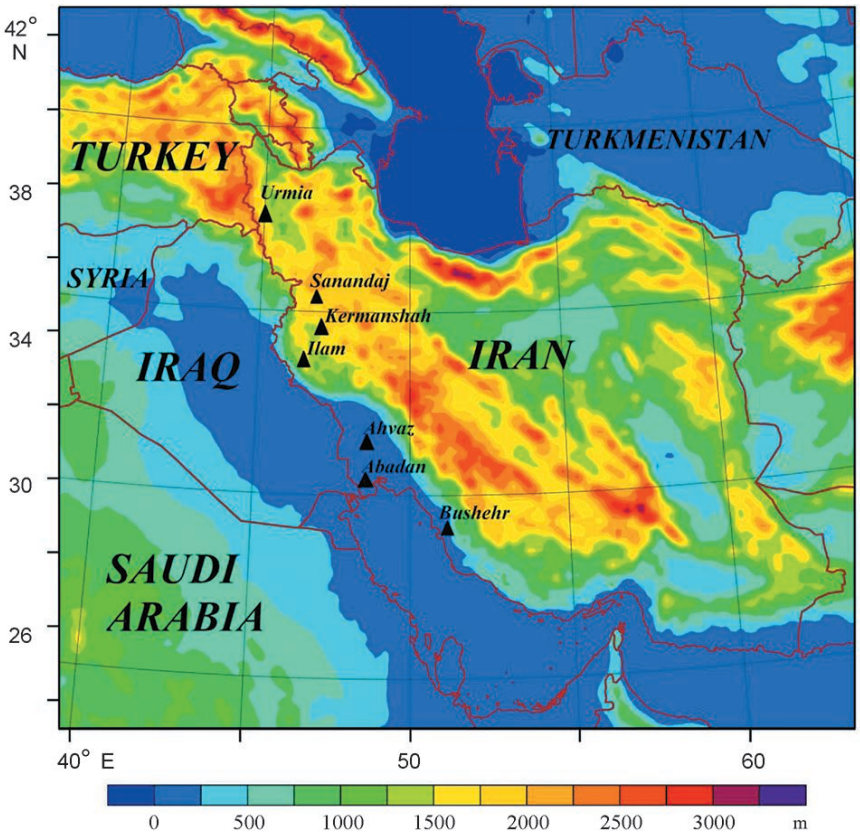

Fig. 1. The topography map of Iran and the location of weather stations considered in this study (the black triangles).

For each station, the frequencies of dust-in-suspension, blowing dust, dust storm and severe dust storm are denoted as f_{DIS}, f_{BD}, f_{DS} and f_{SDS}, respectively. The frequencies are estimated using the synoptic records as follows [25, 26]:

$$f_{DIS} = N_{DIS}/N_{obs}$$

where N_{DIS} is the number of observed dust-in-suspension eventsm, and N_{obs} is the number of synoptic records. The total frequency of dust events f_{DE} is:

$$f_{DE} = f_{DIS} + f_{BD} + f_{DS} + f_{SDS}.$$

Meteorological data for 1990–2013 allow the following conclusions:

—the highest total frequency of dust events is registered at the Bushehr airport station (about 10.70%) and the Ahvaz and Abadan stations (9.9% and 8.5%, respectively);

—the Urmia station has the lowest frequency of dust events (about 1.05%);

—the low amount of dust events exist in the provinces located in the west of Iran (Ilam, Kermanshah, Kurdistan, western Azerbaijan).

Data on the distribution of dust events in the studied region, namely, on their frequency for each class of the WMO classification given above, demonstrate that the highest frequency of dust-in-suspension is observed at Ahvaz station. Dust-in-suspension cases are also observed in the Abadan and Bushehr airport stations but with a lesser frequency. In fact, dust storms and severe dust storms occur rarely in the west and southwest of Iran. The most of the dust events in the west and southwest of Iran are either dust-in-suspension or blowing dust events.

Figure 2a illustrates the annual variation of the total dust events in the west and southwest of Iran. It is seen that dust event frequency had a rapid growth in the west and southwest of Iran. Increase of dust events has been impressive since 2006. The year 2009 was the dustiest year whose total number of dust events was 3221. It is believed that the main reason for the above-mentioned increase in dust occurrence in the region is due to the development of the dam construction projects on the Tigris and Euphrates rivers (e.g.,

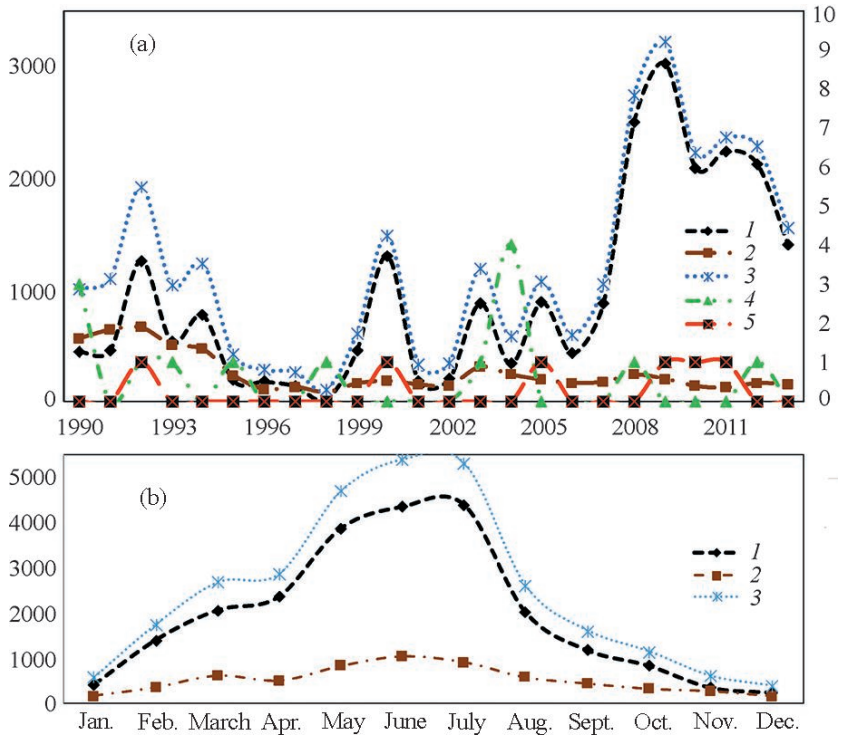

Fig. 2. The frequency of dust events at seven weather stations in the west and southwest of Iran in 1990–2013. (a) Yearly data; (b) mean monthly values. (*1*) dust-in-suspension; (*2*) blowing dust; (*3*) all dust events; (*4*) dust storm; (*5*) severe dust storm.

Guneydoga Anadolu Projesi (GAP) project, the amounts of 14 new dams on the Euphrates and 8 dams on the Tigris) [24]. Construction of new dams decreases soil water content in the downstream area and dry swampland; this consequently lessens the threshold friction velocity of soil and its resistance against wind erosion. Another reason is the decrease of precipitation in recent years [13, 18].

Figure 2b illustrates the monthly variation of dust events in the west and southwest of Iran. Although in the west and southwest of Iran dust events occur in all months of the year, occurrence decreases in November, December, and January, increases in March and April, and reaches the maximum in June, July, and late August.

3. SYNOPTIC ANALYSIS OF CASES

This research analyzes two cases of dust storms that occurred over the west and southwest of Iran on July 4–7, 2009 and June 17–20, 2012. They are among the most severe dust storms recorded in Iran due to their large area coverage and severity. To assess the predictability of the two above mentioned cases, the WRF-Chem numerical model was used to simulate the events.

The western Asia climate is mainly affected by four types of synoptic systems [13]: the Siberian High in winter over central Asia; the monsoon depression in summer over India subcontinent, the south and southeast of Iran and the southeast of the Arabian Peninsula; depressions travelling from northwestern Africa and the southeast of the Mediterranean Sea across the Middle East and the southwest of Asia in spring and winter; the high-pressure ridge associated with the Azores High over Eastern Europe and the Mediterranean Sea.

To elaborate further on the relationship between total dust events and Indian monsoon index, the coefficient of correlation was calculated (–0.49). The total dust events and Indian monsoon index during the period of 1990–2013 are shown in Fig 3. As seen, the highest frequency of total dust events has been reported in 2009 in the region which coincides with a relative minimum in the India monsoon index. However, comprehensive examination of this relationship could be the subject of further studies.

For analyzing the synoptic conditions governing the occurrence of dust, this study uses NCEP/NCAR reanalysis data on sea level pressure, surface wind field, geopotential height at 500 hPa, wind field at 850 hPa, and vertical velocity on July 3–4, 2009 and June 17, 2012.

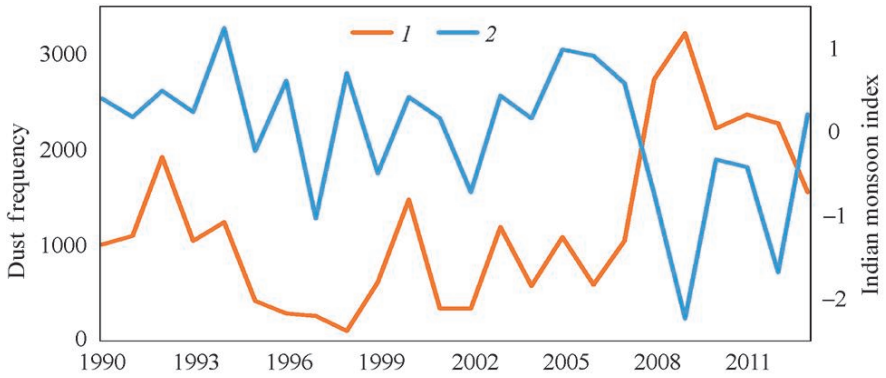

Fig. 3. The time series of (*1*) the Indian monsoon index and (*2*) dust event frequency at seven weather stations in the west and southwest of Iran in 1990–2013.

Figure 4a shows that at 00:00 on July 3, 2009, a low pressure zone with the closed contour of 996 hPa was located at the surface over the Oman Sea and the Persian Gulf. The trough associated with the surface low pressure was oriented from the northwest to the southeast and extended toward the north of Iraq. Also, since a high-pressure center with the 1014 hPa contour line was located in the west of the Caspian Sea, a considerable pressure gradient could be recognized in the northwest of Iran. So, at a relatively small distance of 5 of longitude, the surface pressure differed by 12 hPa. This situation caused strong surface winds in the region. Depending on the type of soil underneath, suitable conditions for a dust event were formed.

In 24 hours the situation changed and the pressure gradient increased over the south of Iraq and east of Syria (15 hPa at 5 of longitude), so favorable conditions for more dust production were provided (see Fig. 4c).

As seen in Fig. 4b, on July 3, 2009, exactly the day before the dust storm, there was a high pressure system over the south of Iran at 500 hPa level and a trough was approaching the west of Syria. Hence, from the east Mediterranean a low-pressure system (the contour value of 5900 gpm) passed through Syria and Iraq, entered Iran, and affected different regions in the west, southwest, south, and center of Iran. A weak upper trough was observed over Syria and Iraq at 500 hPa which indicated the passage of a short-amplitude wave from the northwest of Iran. The main trough system in the lower levels over Europe was located over the center of the Mediterranean (see Fig. 4b).

In 24 hours, the main trough moved further to the east, causing a sharp decrease in the geopotential height over Syria and Iraq (see Fig. 4d). This trough was accompanied with a dynamic low-pressure system at the surface.

In the wind field chart of 850 hPa shown in Fig. 4e, there is a pressure trough extended from the Persian Gulf to Iraq and Syria. The wind speed is in the interval of 9–15 m/s. The maximum of the wind speed (about 12–15 m/s) is seen in the Persian Gulf, Iraq, and the west of Iran. At 00:00 UTC on July 4 there was an increase in the wind speed over Syria and Iraq which indicates favorable synoptic conditions for dust formation (not illustrated).

The positive values of at 500 hPa indicate air downdrafts over Syria, Iraq, and Jordan 2 days before the dust storm events. The Zagros mountain range enforces vertical motions and dust transport to higher altitudes in addition to the horizontal transport which, consequently, decreases the amounts of dust (see Fig. 4f).

In the mean sea level the pressure map for June 17, 2012 (see Fig. 5), a high-pressure system with the closed contour of 1023 hPa is located over Europe. The ridge associated with the above mentioned high pressure is extended from the Black Sea to the north of Iran. So, due to the existence of a low-pressure zone over the south of Iran, there was a strong pressure gradient over the west and north of Iran, the northeast of the Mediterranean Sea and the south of the Black Sea that caused strong winds over the mentioned regions. During the next days, more or less similar conditions maintained, but the pressure gradient was extended to lower latitudes. The pressure gradient over the north of the Mediterranean determined northerly and northeasterly wind directions.

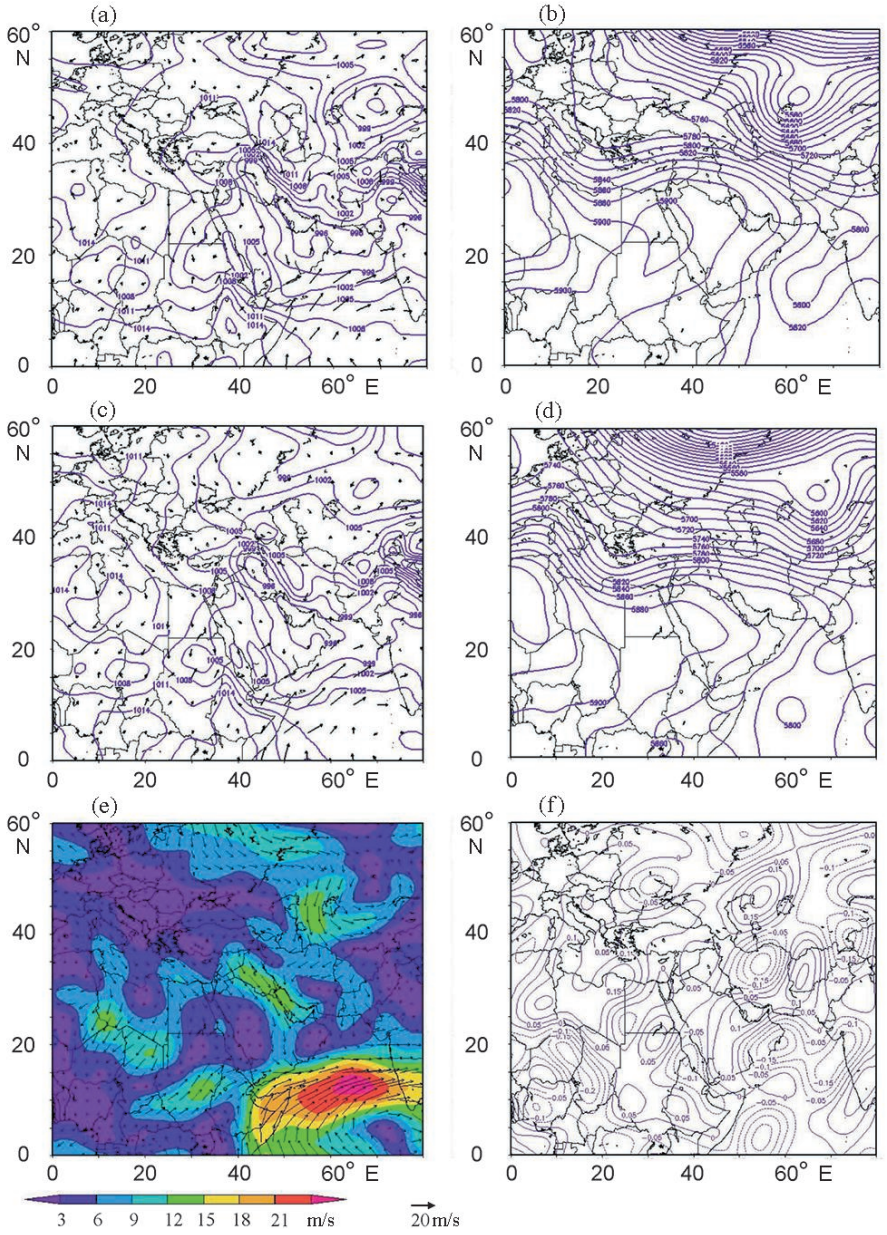

Fig. 4. Sea level pressure, geopotential at 500 hPa, wind field at 850 hPa, and vertical velocity on July 3 and 4, 2009. This figure was created using NCEP/NCAR Reanalysis Data website (http://www.esrl.noaa.gov/psd/data/gridded/data.ncep.reanalysis.html). (a) Sea level pressure (hPa) and wind field (m/s) at 00:00 UTC on July 3, 2009; (b) geopotential at 500 hPa at 00:00 UTC on July 3, 2009; (c) sea level pressure (hPa) and wind field (m/s) at 00:00 UTC on July 4, 2009; (d) geopotential at 500 hPa at 00:00 UTC on July 4, 2009; (e) wind field at 850 hPa at 00:00 UTC on July 3, 2009; (f) the analog of vertical velocity (Pa/s) at 500 hPa at 00:00 UTC on July 3, 2009.

4. SIMULATION OF DUST EVENTS

The present study utilizes version 3.7.1 of the WRF-Chem model [6, 12] to simulate the meteorology and chemistry conditions over the model domain. The chemical part of the model is compiled as a separate program with the main model WRF. It consists of several modules aimed at the modeling and parameterizing chemical processes in the atmosphere.

The ability of the WRF-Chem model to simulate air quality for urban areas is one of the advantages of this model. The model simulates the emission, transport, mixing, and chemical transformation of trace

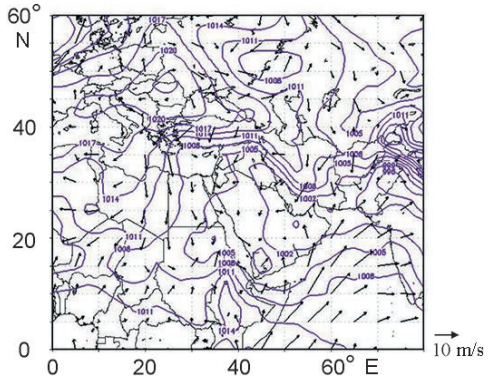

Fig. 5. Sea level pressure on June 17, 2012. This figure was created using NCEP/NCAR Reanalysis Data website (http://www.esrl.noaa.gov/psd/data/gridded/data.ncep.reanalysis.html).

Fig. 6. The model domains.

gases and aerosols simultaneously with the meteorology. The model is used for investigation of regional-scale air quality, field program analysis, and physical and chemical interactions on the cloud scale.

Figure 6 shows the model domains. The model nests are defined on a Mercator projection. Nest 1 extends from 20 to 80 E (98 grid points) and from about 10 to 51 N (90 grid points) at the horizontal grid spacing of 45 45 km, and nest 2 extends from 42 to 70 E (151 grid points) and from about 23.5 to 43 N (139 grid points) at the horizontal grid spacing of 15 15 km. The vertical grid is composed of 27 levels from the surface to 10 hPa (30 km) with a spacing of about 60 m near the surface, 200–400 m for the altitudes of 1–3 km, and 540–600 m for the altitudes of 5–13 km. The static geographical fields, such as terrain, height soil properties, vegetation fraction, land use, and albedo are interpolated from United States Geological Survey (USGS) data with the step of 10 (~19 km) to the model domain; the WRF preprocessing system (WPS) is used.

The model domain encompasses a widely varying landscape with the elevated Zagros and Alborz mountain ranges, the low-altitude (<500 m) Mesopotamian Plains, semi-arid and desert lands, and seashores. The complex terrain in the model domain influences significantly on the meteorology and the distribution of dust.

The initial and lateral boundary conditions for the meteorological fields are obtained from global forecast system (GFS) data with 0.5 0.5 spatial resolution available at National Operational Model Archive & Distribution System (http://nomads.ncdc.noaa.gov/).

The model simulation for the first case was carried out from 00:00 UTC on July 2 to 00:00 UTC on July 8, 2009 at 00:00 UTC. For the second case study, the model simulation lasted from 00:00 UTC June 16

to 00:00 UTC June 21, 2012. For both cases, the model results for the first day were discarded as the model spin up.

Modeling atmospheric aerosols requires the appropriate representations of aerosol dust distribution and microphysics in three-dimensional (3D) air quality models (AQMs). The modal and sectional approaches are the two major approaches commonly used in AQMs to represent the particle size distribution. In the modal approach, the particle size distribution is approximated by several modes, and particle properties are assumed to be uniform in each mode. In the sectional approach, the size distribution is classified in specific sections, and the properties of particulate matters in each section are assumed to be nearly constant. This assumption is necessary for the simplification of the modeling [31].

To calculate aerosols, the WRF-Chem model uses three schemes: Goddard Chemistry Aerosol Radiation and Transport (GOCART) bulk aerosol scheme [5, 20]; the MADE/SORGAM scheme based on the Modal Aerosol Dynamics Model for Europe (MADE) [1] which is a modification of the Regional Particulate Model [14]. Secondary organic aerosols (SOA) have been incorporated into MADE [22] by means of the Secondary Organic Aerosol Model (SORGAM); the Model for Simulating Aerosol Interactions and Chemistry (MOSAIC) [30]. This study uses and compares only two schemes, GOCART (a simple aerosol scheme, no ozone chemistry, plus a scheme based on RADM2 Chemistry and GOCART aerosols) and MADE/SORGAM. Gas-phase chemistry is represented by the Regional Acid Deposition Model of the second generation (RADM2) [28]. To describe the physics of atmospheric processes, the WRF-Chem model uses the Morrison two-moment scheme; to calculate long-wave and short-wave radiation, RRTMG scheme; to estimate the surface layer depth, the Monin–Obukhov parameter; to describe the underlying surface, the Hoah parameterization scheme. The boundary layer is described using the YSU scheme, and cumulus clouds, using the Grell-3 scheme.

In the Middle East, due to its climatic conditions with poor vegetation cover and 92–97% share in the total mass of particles PM_{10}, dust particles emitted from the field of organic (biogenic) matter are ignored by the model.

5. RESULTS AND DISCUSSION

As discussed in Section 3, on July 3–4, 2009 the formation of a low-pressure system over the region and the development of unstable conditions over Syria and Iraq as well as the effect of dynamic low pressure area created favorable conditions for dust formation and, consequently, caused the propagation of large quantity of dust particles over the southwest, south, and west of Iran.

As mentioned earlier, we used two dust schemes of GOCART (with Kinetic Preprocessor KPP and without it) and MADE/SORGAM in the simulations. The KPP [11] is used in WRF-Chem as a chemical solver tool which consumes less time than the manual coding and is more numerically efficient. Simulated PM_{10} values for Ahwaz station are compared with the corresponding observed values.

As seen in Fig. 7a, the MADE/SORGAM scheme shows relatively better performance compared to GOCART, and the values and trends of PM_{10} are better predicted. On July 4, 2009, the measured average amount of PM_{10} was 3125 g/m^3, and the corresponding simulated value was 2351 g/m^3. Afterwards, the rate of decrease during the simulation was significantly lower than during the observation.

Figure 7b shows the observed and simulated time series of PM_{10} for dust storms that occurred on June 16–21, 2012 at Ahvaz station. As seen, the MADE/SORGAM scheme had better performance than the GOCART scheme for configurations with and without KPP. MADE/SORGAM scheme estimates both the trend and the value of simulated PM_{10} with an acceptable accuracy, while the estimations of PM_{10} by the other two schemes are poor. In this dust event, the maximum PM_{10} the maximum PM_{10} value recorded in Ahvaz station on June 19, 2012 is 2290 g/m^3, and its corresponding simulated value calculated using the MADE/SORGAM scheme is 2622.77 g/m^3.

According to model calculations, on July 3, 2009 there was a low-pressure area in the north of Iraq, easterly currents in Turkey, southerly currents in the northeast of Syria, and northwesterly currents in the north of Iraq (no figures are presented). The WRF-Chem outputs indicate that this low-pressure area motion is synchronized with the northwesterly currents over Syria and causes their propagation over Iraq and the north of Persian Gulf. Also, dust particles are predicted in the north of Iraq, northwest of Iran and east of Syria. Moreover, at the same time there is dust in the east and center of Iran; also the model simulates dust in the Ghareghom Desert of Turkmenistan.

Twelve hours later, at 12:00 UTC on July 3, 2009, the model shows that wind speed increases over Iraq, Syria, and the most parts in the west of Iran that consequently causes dust in central Syria. At the same time, there are northwesterly winds over Iraq directed towards the north of the Persian Gulf. Westerly winds

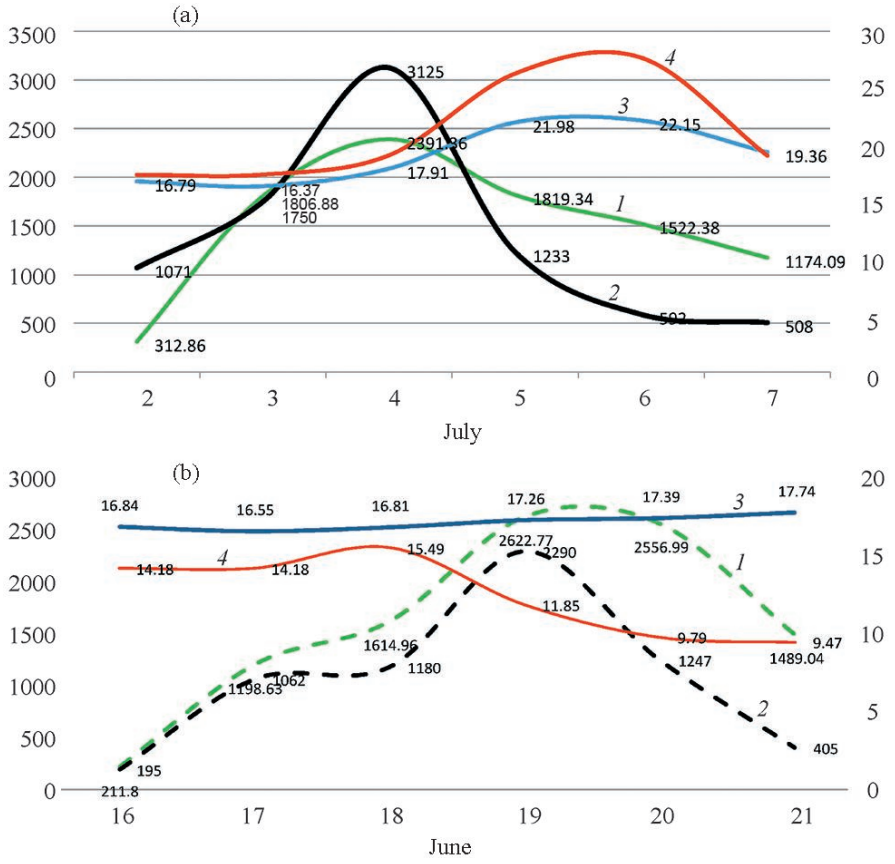

Fig. 7. Time series of PM_{10} during severe dust storms at Ahvaz station (a) on July 3–9, 2009 and (b) on June 16–21, 2012. (*1*) the values calculated with the MADE/SORGAM scheme; (*2*) observational data; (*3*) calculation by the GOCART scheme without KPP; (*4*) calculation by the GOCART scheme with KPP.

blow from the north of Iraq towards the western provinces of Iran. Also, increase in the wind speed in the eastern half of Iran causes wind direction changes from northerly to easterly. Therefore, convergent currents are formed along the Zagros Mountains; this causes dust to move towards the convergent region (the Zagros Mountains). The model predicts dust in the eastern parts of the Zagros Mountains and also over Khuzestan and Ilam provinces that are located in the southwest of this mountain range. This dust is partly originated from the central deserts of Iran and partly from the eastern regions of Iraq.

The simulated dust at 00:00 UTC is less than at 12:00 UTC because of the decrease in the temperature and increase in the relative humidity and adherence of soil particles over the Earth surface. Increase in temperature and decrease in relative humidity causes dust storm in the region.

By 00:00 UTC on July 4 conditions of dust formation over Iraq are predicted again, so that the wind direction over Iraq causes dust to move towards the west of Iran. This situation continues 12 hours later, and dust amount increases in the north and northwest of Iran, Ilam, Khuzestan, and Bushehr provinces.

The predicted maximum dust concentration over the central parts of Iraq and the coasts of the Persian Gulf in Bushehr and Hormozgan provinces is the result of the dust that was observed earlier. Examination of the results shows that in the desert areas (mountainous regions) the boundary layer height increases between 06:30 and 12:00 UTC and concentration decreases (increases) accordingly. The model successfully simulates the boundary layer height evolution. As the model successfully simulates the formation of synoptic systems over the Mediterranean and its further development over the west and northwest of Iran, associated dust concentrations are also successfully predicted.

Examining the 10-meter wind field on June 17–20, 2012 shows that northerly and northeasterly wind is created over the north of Syria. This situation almost coincides with wind speed field in the synoptic maps, and this condition causes dust distribution in the region. Since in northern Syria the wind flow is

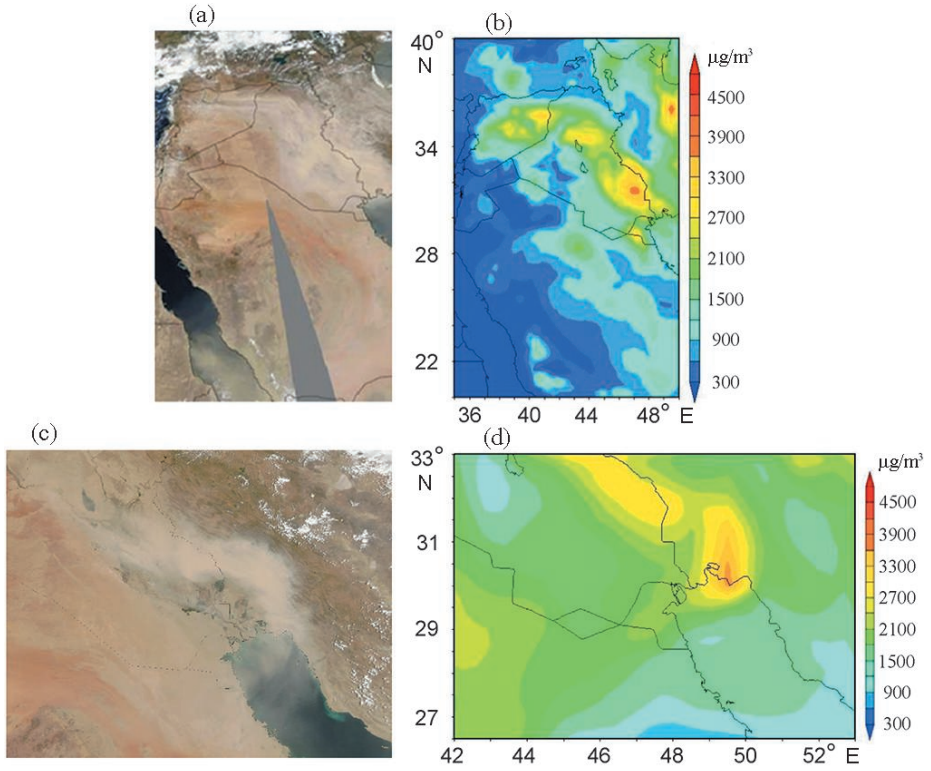

Fig. 8. (a, c) The images in natural colors captured by the Moderate Resolution Imaging Spectroradiometer (MODIS) aboard the Aqua satellite and (b, d) the spatial distribution of column integrated PM_{10} simulated by WRF-Chem for the subregional model domain (a, b) on July 4, 2009 and (c, d) on June 18, 2012.

directed towards the north of the Mediterranean Sea and southern Syria, dust propagates both in western and southern directions.

Also, due to the low-pressure trough associated with the thermal low located over the south of the Persian Gulf and extending toward the Zagros Mountains in the west of Iran, there are easterly winds in the northern part of the trough in the center and west of Iran. These regions suffer from prolonged drought, so producing favorable conditions for dust formation.

The numerical model results show that dust is formed over the deserts of central Iran and moves towards the western provinces of the country. Increased wind speed increases dust amount and its area coverage.

The simulated wind speed in the east of Turkey is faster compared to its value 12 hours later. Thus, with increase of wind speed, wind direction is also changed due to the strengthening or weakening of cyclonic and anticyclonic flow. Obviously, these changes cause increase in dust amount in the region so that it covers a wider area. As the wind speed gradually increases (until June 17, 2012 at 18:00 UTC), the dust is transferred to the northern part of the Mediterranean Sea and also involves the northern, southern, and central regions of Syria.

The model results for the coming days (June 18 and 19, 2012) show that a wider area in the Mediterranean Sea, west of Iraq, and east of Jordan is in the zone of intensive horizontal spread of dust. The model results show that from 18:00 UTC on June 12, 2012 the low-pressure center appears to the west and northwest of Iran and causes moderately strong wind shear over the region. These conditions gradually develop, according to the model, and the northwesterly winds over Iraq cause dust in the eastern part of Iraq. Thus, a large area of the western provinces of Iran including Kurdistan, Ilam, Khuzestan, and Kermanshah are affected by dust. This condition continues until 19 June, the low-pressure center moves to the lower latitudes, and a wall of dust is predicted around the center of this zone. Also, the model shows that wind speed increases in the eastern regions of Zagros, and dust amount increases too.

On June 20 over the west of Iran, the wind speed decreased, but due to the existence of a low-pressure area over the region, there still were favorable conditions for dust formation. Easterly winds cause this situ-

ation to be extended over Iraq, as a result, westerly and northwesterly currents enter Iran from the west and northwest.

Figure 8 shows the observed and corresponding simulated values of column integrated PM_{10} over Iran. Natural colors in the images captured by MODIS on July 4, 2009 (Fig. 8a) and June 18, 2012 (Fig. 8b) show an event of dust blowing through the west and southwest of Iran. Comparison of the spatial pattern of the dust plume produced by WRF-Chem with MODIS images shows that the simulated pattern agrees well with the observed one. Both MODIS and WRF-Chem results for July 4, 2009 (Fig. 8c) and June 18, 2012 (Fig. 8d) show that dust blew along the Iraq–Iran border and the direction changed from west–east to northwest–southeast and to northeast–southwest, respectively.

A comparison of satellite images for the dust storm event with simulations by the WRF-Chem model suggests that the model has a good ability to reproduce the spatial pattern of PM_{10} particulate emissions.

REFERENCES

1. I. J. Ackermann et al., "Modal Aerosol Dynamics Model for Europe: Development and First Applications," Atmos. Environ., No. 17, **32** (1998).
2. R. Arimoto et al., "Trace Elements in the Atmosphere over the North Atlantic," J. Geophys. Res. Atmos., No. D1, **100** (1995).
3. A. Baklanov et al., "Online Coupled Regional Meteorology Chemistry Models in Europe: Current Status and Prospects," Atmos. Chem. and Phys., No. 1, **14** (2014).
4. F. S. Binkowski and U. Shankar, "The Regional Particulate Matter Model: 1. Model Description and Preliminary Results," J. Geophys. Res. Atmos., No. D12, **100** (1995).
5. M. Chin et al., "Tropospheric Aerosol Optical Thickness from the GOCART Model and Comparisons with Satellite and Sun Photometer Measurements," J. Atmos. Sci., No. 3, **59** (2002).
6. K. Fast et al., "Ozone Abundance on Mars from Infrared Heterodyne Spectra: II. Validating Photochemical Models," Icarus, No. 2, **183** (2002).
7. H. K. H. Furman, "Dust Storms in the Middle East: Sources of Origin and Their Temporal Characteristics," Indoor and Built Environ., No. 6, **12** (2003).
8. J. Ge et al., "Dust Aerosol Optical Properties Retrieval and Radiative Forcing over Northwestern China during the 2008 China/US Joint Field Experiment," J. Geophys. Res. Atmos., No. D7, **115** (2010).
9. H. Gerivani et al., "The Source of Dust Storm in Iran: a Case Study Based on Geological Information and Rainfall Data," Carpat. J. Earth and Environ. Sci., No. 6 (2011).
10. A. Goudie and N. Middleton, "Saharan Dust Storms: Nature and Consequences," Earth-Sci. Rev., No. 1, **56** (2001).
11. G. Grell and A. Baklanov, "Integrated Modeling for Forecasting Weather and Air Quality: A Call for Fully Coupled Approaches," Atmos. Environ., No. 38, **45** (2011).
12. G. A. Grell et al., "Fully Coupled "Online" Chemistry within the WRF Model," Atmos. Environ., No. 37, **39** (2005).
13. M. Hamidi et al., "Synoptic Analysis of Dust Storms in the Middle East," Asia Pacific J. Atmos. Sci., No. 4, **49** (2013).
14. J. Haywood and O. Boucher, "Estimates of the Direct and Indirect Radiative Forcing due to Tropospheric Aerosols: A Review," Rev. Geophys., No. 4, **38** (2000).
15. J. F. Leon and M. Legrand, "Mineral Dust Sources in the Surroundings of the North Indian Ocean," Geophys. Res. Lett., No. 6, **30** (2003).
16. N. Middleton, "Dust Storms in the Middle East," J. Arid Environ., 1986.
17. N. Middleton et al., "The Frequency and Source Areas of Dust Storms," Aeolian Geomorphol., **23** (1986).
18. M. Miri et al., "Spatial Analysis and Source Identification of PM_{10} Particle Matter in Yazd," JCHR, No. 1, **5** (2016).
19. S. U. Park and H. J. In, "Parameterization of Dust Emission for the Simulation of the Yellow Sand (Asian Dust) Event Observed in March 2002 in Korea," J. Geophys. Res. Atmos., No. D19, **108** (2003).
20. G. Pfister et al., "Characterizing Summertime Chemical Boundary Conditions for Airmasses Entering the US West Coast," Atmos. Chem. and Phys., No. 4, **11** (2011).
21. S. Satheesh and K. K. Moorthy, "Radiative Effects of Natural Aerosols: A Review," Atmos. Environ., No. 11, **39** (2005).
22. B. Schell et al., "Modeling the Formation of Secondary Organic Aerosol within a Comprehensive Air Quality Model System," J. Geophys. Res. Atmos., No. D22, **106** (2001).
23. J. H. Seinfeld et al., "ACE-ASIA: Regional Climatic and Atmospheric Chemical Effects of Asian Dust and Pollution," Bull. Amer. Meteorol. Soc., No. 3, **85** (2004).

24. A. Shahsavani et al., "The Evaluation of PM10, PM2.5, and PM1 Concentrations during the Middle Eastern Dust (MED) Events in Ahvaz, Iran, from April through September 2010," J. Arid Environ., **77** (2012).
25. Y. Shao and C. Dong, "A Review on East Asian Dust Storm Climate, Modeling, and Monitoring," Global and Planetary Change No. 1, **52** (2006).
26. Y. Shao and J. Wang, "A Climatology of Northeast Asian Dust Events," Meteorol. Zeitschrift No. 4, **12** (2003).
27. W. C. Skamarock et al., "A Multiscale Nonhydrostatic Atmospheric Model Using Centroidal Voronoi Tesselations and C-grid Staggering," Mon. Wea. Rev., No. 9, **140** (2012).
28. W. R. Stockwell et al., "The Second Generation Regional Acid Deposition Model Chemical Mechanism for Regional Air Quality Modeling," J. Geophys. Res. Atmos., No. D10, **95** (1990).
29. A. Zakey et al., "Implementation and Testing of a Desert Dust Module in a Regional Climate Model," Atmos. Chem. and Phys., No. 12, **6** (2006).
30. R. A. Zaveri et al., "Model for Simulating Aerosol Interactions and Chemistry (MOSAIC)," J. Geophys. Res. Atmos., No. D13, **113** (2008).
31. Y. Zhang et al., "Regional Integrated Experiments on Air Quality over Pearl River Delta 2004 (PRIDE-PRD2004): Overview," Atmos. Environ., No. 25, **42** (2008).
32. Z.-K. Zhang et al., "Solving the Cold-start Problem in Recommender Systems with Social Tags," EPL (Europhysics Letters), No. 2, **92** (2010).
33. C. Zhao et al., "Radiative Impact of Mineral Dust on Monsoon Precipitation Variability over West Africa," Atmos. Chem. and Phys., No. 5, **11** (2011).
34. M. Zoljoodi and A. Didevarasl, "Evaluation of Spatial-temporal Variability of Drought Events in Iran Using Palmer Drought Severity Index and Its Principal Factors (through 1951–2005)," Atmos. and Climate Sci., No. 2, **3** (2013).